ISSN 2411-3336; e-ISSN 2541-9404

JOURNAL OF MINING INSTITUTE

Zapiski Gornogo instituta

Journal homepage: pmi.spmi.ru

Research article
UDC 553.9+553.21

Ti-Fe-Cr spinels in layered (stratified) complexes of the western slope of the Southern Urals: species diversity and formation conditions

Sergey G. KOVALEV ✉, **Sergey S. KOVALEV**
Institute of Geology, Ufa Scientific Centre RAS, Ufa, Russia

***How to cite this article*:** Kovalev S.G., Kovalev S.S. Ti-Fe-Cr spinels in layered (stratified) complexes of the western slope of the Southern Urals: species diversity and formation conditions. Journal of Mining Institute. 2022. Vol. 255, p. 476-492. DOI: 10.31897/PMI.2022.54

Abstract. Materials on geochemistry and ore Fe-Ti-Cr mineralization of rocks composing layered (stratified) bodies of the western slope of the Southern Urals are presented. A detailed analysis showed similarity in the redistribution of REE, noble metals, and Fe-Ti-Cr mineralization of practically all parameters in rocks of the Misaelga and Kusin-Kopan complexes. It has been established that the parameters of metamorphism, which influenced components redistribution in Fe-Ti-Cr minerals of the layered complexes, correspond to Misaelga – T = <550-750 °C, P = 0.1-2.8 kbar, Kusin-Kopan – T = <550-630 °C, P = 0.3-0.7 kbar, and Shuidinsky complexes – T = <550-760 °C, P = 0.5-2.5 kbar. The result of modelling the melt crystallization process showed that the Kusin-Kopan complex is an intrusive body with an ultramafic horizon in the idealized cross-section. Due to collisional processes, the lower part of the intrusion has been detached from the upper part. The proposed structure of the Kusin-Kopan complex sharply increases its prospects for such types of minerals as platinum group minerals + sulphide copper-nickel mineralization and/or chromites.

***Keywords*:** Southern Urals; layered (stratified) complexes; Fe-Ti-Cr mineralization; rare earth elements; noble metals

Acknowledgments. This work was carried out within the framework of the State Assignment (Theme N FMRS-2022-0012).

***Received*: 21.03.2022** ***Accepted*: 15.06.2022** ***Online*: 26.07.2022** ***Published*: 26.07.2022**

Introduction. The family of chromspinels is characterized by cubic syngony and widely manifested isomorphism in the series $MgAl_2O_4$-$FeAl_2O_4$, $MgAl_2O_4$-$MgCr_2O_4$, $MgAl_2O_4$-$FeCr_2O_4$. Almost all members of these series are ore minerals, industrially important deposits of iron, iron-titanium, and chromite ores. This paper considers the formation of titaniferous magnetite mineralization in layered intrusions located on the western slope of the Southern Urals.

Currently, deposits of titaniferous magnetite ores are developed practically on all continents. They are known in China, South Africa, Tanzania, Norway, Sweden, the USA, and other countries. Most of the objects are localized in layered syenite-gabbro, gabbro-anorthosite, and dolerite-picrite complexes. In Russia, deposits of titaniferous magnetite ores have been identified in Siberia, the Far East, Karelia, and the Kola Peninsula. The Ural region is a classic area of titaniferous magnetite deposits, these objects are confined to dunite-pyroxenite-gabbro formation – Kachkanar, Pervouralsk, Visim, Suroyamsk, Velikhov, Tebinbulak, Gusevogorsk [1], stratified basic-ultrabasic intrusions – Kusin-Kopan group of deposits (Kusin, Kopan, Medvedev, Matkalsk, Chernorechensk) [2, 3] as well as numerous ore occurrences, which prospects are not clear because they are poorly studied (Yubrishkinsk and others) [4].

According to most researchers, titaniferous magnetite mineralization in layered complexes has a magmatic origin and is caused by the formation of intrusive massifs [5]. At the same time, the mechanisms of ore-forming processes are the subject of heated discussions. In particular, the models of gravitational accumulation of magnetite (titaniferous magnetite) and ilmenite [6, 7], ore melt liquation [8-12] are actively developed, and "combination" models, in which the formation of Fe-Ti mineralization is caused by a special mechanism of silicate minerals crystallization, are actively discussed [13].

The paper aims to characterize Ti-Fe-Cr mineralization in various layered (stratified) complexes located on the western slope of the Southern Urals, reconstruct conditions of its formation, and construct a model of the geological structure of the Kusin-Kopan complex.

Methodology. Mineral compositions were studied using a scanning electron microscope REMMA-202M with an X-ray energy dispersive spectrometer LZ-5 (SiLi detector, 140 eV resolution) and detectors of secondary (SE) and reflected (COOMPO) electrons at the Institute of Mineralogy UB RAS (Miass, analyst V.A.Kotlyarov). In carrying out quantitative point analysis accelerating voltage of 20-30 kV at probe currents of 4 to 6 nA was used. When analyzing the composition of minerals, pure metal standards or synthetic (natural) minerals were used.

The compositions of minerals of the Kusin-Kopan complex were studied on a scanning electron microscope Tescan Vega Compact with energy dispersive analyzer Xplorer Oxford Instruments (GI UFRC RAS, Ufa). The following settings were used: accelerating voltage 20 kV, probe current 4 nA, spectral accumulation time in the Point&ID mode 60 sec, beam diameter ~3 μm. An integrated set of Oxford Instruments Standards standards, represented by natural and synthetic compounds, was used in the analysis.

Concentrations of petrogenic components were determined by the XRD method in GI UFRC RAS (Ufa) using the spectrometer VRA-30 ("Carl Zeiss", Germany). Detection limits for SiO_2 and Al_2O_3 were 0.1 % (here and further elements in wt.%), TiO_2, Fe_2O_3, MnO, CaO, K_2O, P_2O_5 and S_{total} – 0.01 %, MgO – 0.2 %.

REE concentrations were determined by ICP-MS at Isotope Centre (Russian Geological Research Institute, VSEGEI, St. Petersburg). Quantitative determination of noble metal content (Au, Pt, Pd, Rh, Ru, Ir) was also carried out at VSEGEI Isotope Centre (St. Petersburg).

Discussion. *The Shuidinsky complex* is located in the central part of the Bashkirian meganticlinorium among the Lower Triassic sediments (Fig.1). It combines asymmetrically and symmetrically layered bodies of variable (15-30 m) thickness. The asymmetrically constructed sill with a thickness of about 30 m has been studied in a natural outcrop [4]. It is composed of olivine clinopyroxenite, olivine websterite, dipyroxene gabbro-dolerite and is characterized by two horizons: the upper (basic) and lower (ultrabasic).

Ultrabasic horizon is represented by olivine clinopyroxenite, olivine websterite with porphyritic structure, consisting of subidiomorphic olivine crystals, elongated prismatic precipitations of orthopyroxene, clusters, and individual crystals of clinopyroxene with various degrees of idiomorphism, as well as amphibole, plagioclase, magnetite, chromspinel, ilmenite, sulphides and apatite.

The lower part of the upper horizon is composed of websterite, which changes upwards through the intermediate variations to dipyroxene gabbro-dolerites and their leucocratic varieties.

The Misaelga complex has been identified in the southern part of the Taratashsky metamorphic complex [2, 14, 15]. Its composition includes porphyritic olivine dolerite (in the endocontact zones), medium-grained olivine pyroxenite, gabbro-dolerite, and ferrogabbro-dolerite. The intrusive is distinguished (from bottom to top): lower endocontact zone (about 2 m), ultrabasic horizon (110-112 m), and gabbro horizon (100-110 m).

Journal of Mining Institute. 2022. Vol. 255. P. 476-492
DOI: 10.31897/PMI.2022.54

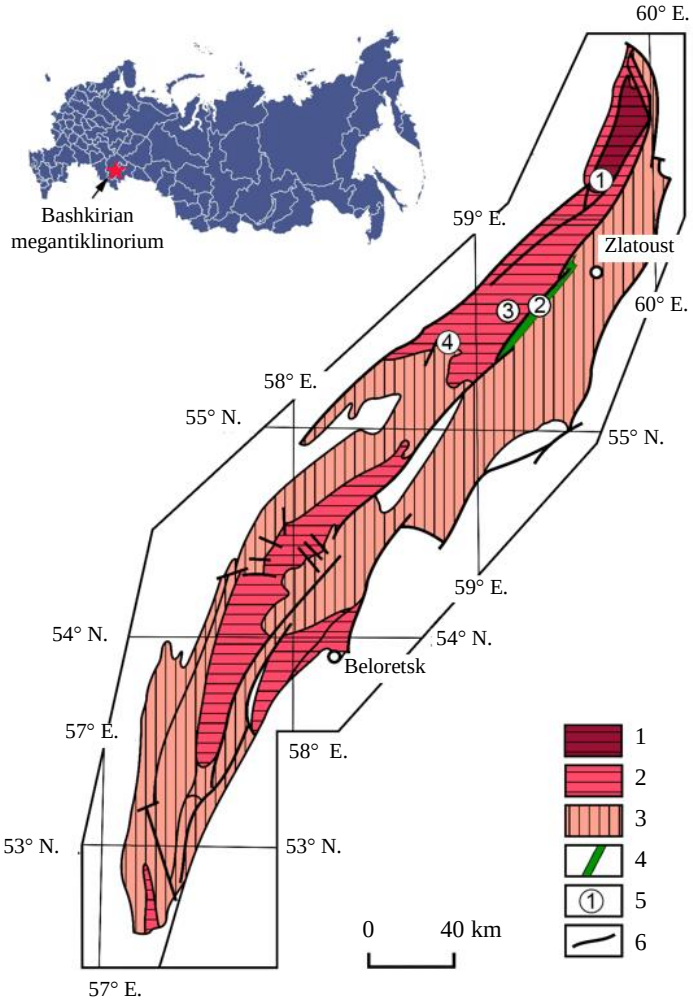

Fig.1. Geological scheme of the Bashkirian megantiklinorium and distribution of layered complexes

1 – AR-PR sediments not dissected; 2 – RF_1 sediments; 3 – RF_2 sediments; 4 – Middle Riphean volcanic-intrusive formations; 5 – layered complexes (1 and 2 – Misaelga and Kusin-Kopan complexes; 3 – rocks of borehole N 7; 4 – Shuidinsky complex); 6 – tectonic boundaries

The lower endocontact zone is composed of medium-grained porphyritic olivine dolerites, the mineral composition of which includes: olivine, orthopyroxene, clinopyroxene, plagioclase, amphibole, biotite, magnetite, titaniferous magnetite, ilmenite, sulphides, apatite, and titanite.

The ultramafic horizon is represented by medium-grained olivine pyroxenite and websterite, which mineral composition varies depending on the location in the section. The rocks consist of olivine, orthopyroxene, clinopyroxene, plagioclase, biotite, magnetite, ilmenite (picroilmenite), chromspinel (Cr-magnetite), and sulphides.

The gabbro horizon is composed of typical gabbro, ferrogabbro-dolerites, their more leucocratic varieties to veined plagiogranite. The mineral composition includes clinopyroxene, plagioclase, amphibole, biotite, magnetite, Ti-magnetite, and sulphides. In the near-vein part of the intrusion, veins of plagiogranite composition are recorded, which are the most acidic derivates of the magma that formed the intrusion.

The layered body of the Borehole N 7. The Borehole is located to the west (~1 km) of the eastern contact of the Kopan massif of the Kusin-Kopan complex. The layered body section uncovered by the borehole has the following structure [16]: 0-38.3 m – limestone (intensely calcified in the exocontact zone); 38.3-101.7 m – layered body with the following horizons (from top to bottom of the section): endocontact zone, represented by fine-grained olivine-containing pyroxenite; below, there is a horizon of taxitic gabbro, which is gradually replaced by olivine gabbro with 10-20 % olivine. The mineral composition of the rocks includes olivine, orthopyroxene (rare), clinopyroxene, plagioclase, amphibole, biotite, magnetite (chromspinel), titaniferous magnetite, sulphides, apatite, and titanite.

The Kusin-Kopan complex is one of the best-known associations of layered (stratified) intrusive rocks of the Southern Urals. The complex consists of several separate massifs (Kusin-Chernorechensk, Medvedev, Kopan, and Matkala), extending in the submeridional direction for a distance of about 70 km with a total area of about 50 km^2 [2]. The internal structure of individual massifs is characterized by a banded structure, due to the alternation of interlayers of gabbro series of variable thickness, different composition, structure, and texture. In addition, the banding is emphasized by the presence of consonant layers of disseminated and continuous titaniferous magnetite-ilmenite ores. The massifs are composed of basic rocks, diverse in composition and structure. Pyroxenites, hornblendites, and anorthosite are of subordinate importance. The rocks composing the banded series

consist of plagioclase (labrador), clinopyroxene (augite) of variable composition, magnesian hypersthene and olivine (chrysolite) are rare, amphibole, biotite, and sulphides are present in small quantities. Pyroxenites have been established in the Matkala and Medvedev massifs. Clinopyroxene is completely replaced by amphibole or by an association of magnesian amphibole – chlorite. Acidic derivates are represented by diorite granite rocks, located in the south-eastern part of the Kopan, Medvedev, and Matkala massifs as a band up to 400-700 m wide. Their internal structure is an interlacing of diorites, granodiorites, and granites. Attribution of granites of the Ryabinov massif to the stratified series is problematic. Detailed arguments are given in [2].

The geochemical characteristics of the rocks emphasize the peculiarities of their geological structure. As can be seen from the classification SiO_2 – Na_2O + K_2O diagram (Fig.2, *a*), the maximum number of diverse products of differentiation is characteristic of rocks of the Kusin-Kopan and Misaelga complexes. In the medium and acid rock varieties some silica deficit is fixed, but generally for rocks of both complexes differentiation has the following direction: pyroxenite → leucocratic granite. The trend of rock basicity change during differentiation, characterizing the Shuidinsky complex, is classical – the concentration of silica increases in the late varieties, and the differentiation changes from pyroxenite to diorite without intermediate varieties. Even more contrasting differences in geochemical characteristics of the complexes are revealed on the AFM diagram (Fig.2, *b*), where rocks of the Kusin-Kopan, Misaelga complexes, and the body of borehole N 7 are characterized by the tholeiite (Fennerian) trend, whereas rocks of the Shuidinsky complex are characterized by the lime-alkali (Bowenian) differentiation trend.

The REE distribution is characterized by a certain peculiarity. In rocks of Misaelga complex degree of REE fractionation (average for gabbro group – La_n/Lu_n – 10.7, Ce_n/Yb_n – 9.1; for pyroxenites – 8.2, 7.3, respectively), as well as the fractionation of light (La_n/Sm_n for gabbro group – 2.2, pyroxenites – 2.0) and heavy (Gd_n/Yb_n for gabbro group – 3.28, for pyroxenites – 3.06) REE indicates their "inert" behaviour at melt differentiation inside the chamber (Fig.2, *c*, *d*). Only at final stages, the residual melt is sharply enriched by the entire REE group.

In rocks of the Kusin-Kopan complex, normalized REE distribution and their fractionation degree are close to those described above (Fig.2, *c*, *d*). So, fractionation parameters for olivine gabbro-norites – La_n/Lu_n – 4.59, Ce_n/Yb_n – 4.06; gabbro-norites La_n/Lu_n – 5.2, Ce_n/Yb_n – 4.79 and granodiorites – La_n/Lu_n – 4.58, Ce_n/Yb_n – 5.1 are close to each other and only in anorthosite they rise to: La_n/Lu_n – 14.15, Ce_n/Yb_n – 10.63. At the same time, fractionation of light (La_n/Sm_n for olivine gabbro-norites – 1.93, gabbro-norites – 1.52, granodiorites – 2.25 and anorthosite – 3.04) and heavy (Gd_n/Yb_n for olivine gabbro-norites – 1.83, 2.36, granodiorite – 1.28, and anorthosite – 2.83) REE are also close to each other, that testifies to coherent behavior of REE during magmatic differentiation.

For pyroxenites from the Borehole N 7 differing from each other by the presence/absence of olivine, the normalized REE distribution is close to that of rocks of Misaelga and Kusin-Kopan complexes (Fig.2, *c*, *d*), but differentiation coefficients are completely equivalent (pyroxenites La_n/Lu_n – 9.14, Ce_n/Yb_n – 7.15; olivine pyroxenites – La_n/Lu_n – 9.92, Ce_n/Yb_n – 7.57; La_n/Sm_n 2.4-2.33; Gd_n/Yb_n 2.54-2.8, respectively).

Normalized REE distribution in rocks of the Shuidinsky complex is sharply different from the rocks characterized above (Fig.2, *c*, *d*). If REE distribution and differentiation parameters in gabbro group (La_n/Lu_n – 7.94; Ce_n/Yb_n – 6.2; La_n/Sm_n – 2.99; Gd_n/Yb_n – 1.77) are close to counterparts from other complexes, then the rocks of ultrabasic horizon differ greatly in quantitative characteristics (see Fig.2, *d*), and differentiation coefficients of REE (La_n/Lu_n – 1.91; Ce_n/Yb_n – 1.75; La_n/Sm_n – 1.46; Gd_n/Yb_n – 1.13).

Journal of Mining Institute. 2022. Vol. 255. P. 476-492
DOI: 10.31897/PMI.2022.54

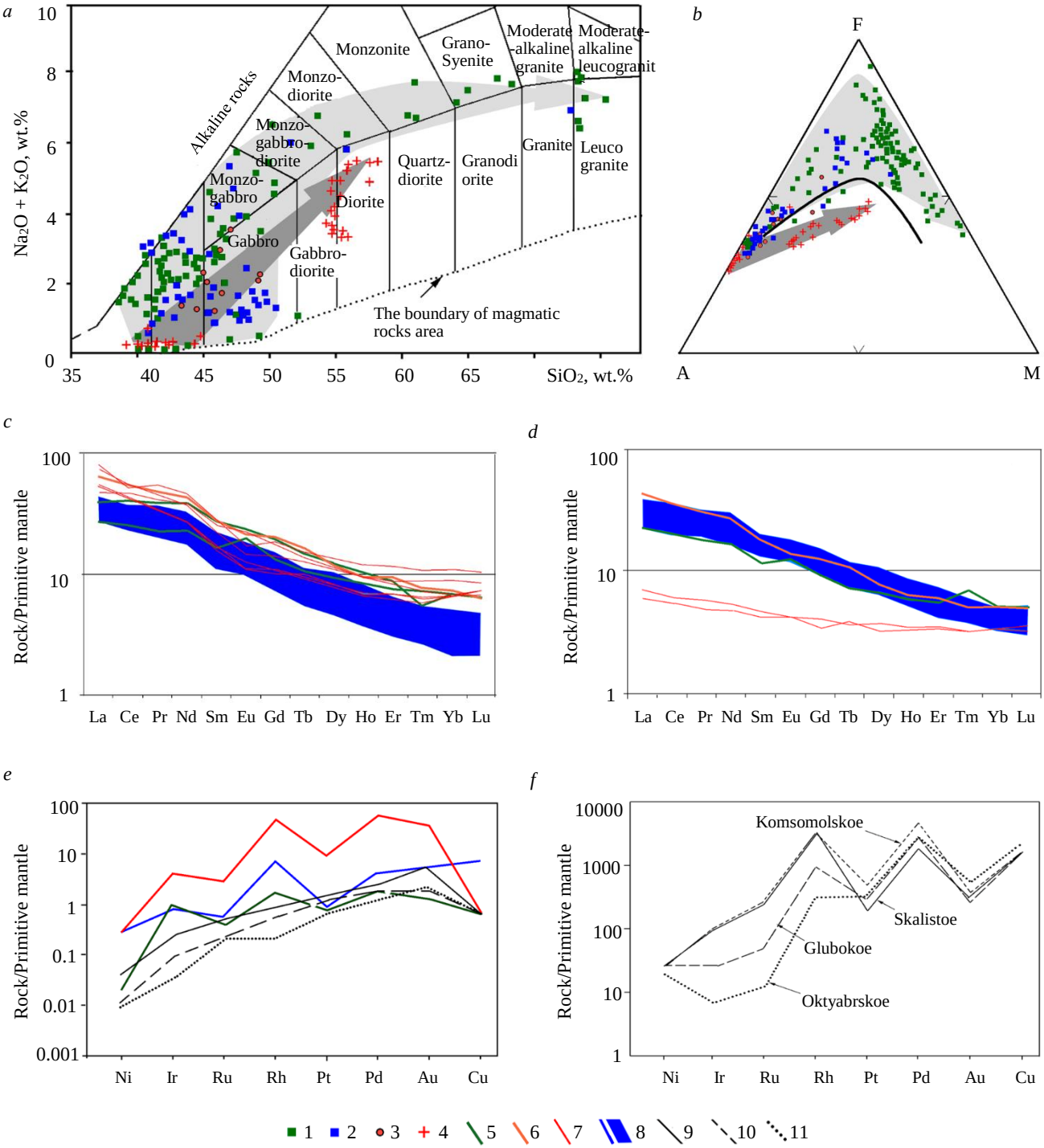

Fig.2. Geochemical diagrams for layered (stratified) complexes of the western slope of the Southern Urals
Diagrams: *a* according to [17]; *b* according to [18]; *c* – for the main rock varieties; *d* – ultrabasic rocks; *e*, *f* – according to [19].
1 and 2 – Kusin-Kopan and Misaelga complexes; 3 – Borehole N 7; 4 – Shuidinsky complex.
The dark gray arrow indicates the direction of differentiation in rocks of the Shuidinsky complex, light gray arrow indicates the direction of differentiation in rocks of the Misaelga and Kusin-Kopan complexes; 5 – Kusin-Kopan complex; 6 – Borehole N 7 complex; 7 – Shuidinsky complex; 8 – Misaelga complex; 9 – average composition of picrites [20];
10 and 11 – according to [19]: Norilsk ore-bearing rocks (10), continental tholeiite (11); primitive mantle according to [21]

Thus, the normalized REE distribution in rocks and their differentiation indicators emphasize the similarity of REE behaviour in rocks of the Misaelga, Kusin-Kopan, and the Borehole N 7 complexes, on the one hand, and the analogues in basicity composing the Shuidinsky complex, on the other hand.

The analysis of noble metal content and distribution is of some interest. Peculiarities of noble-metal geochemical specialization of rocks are revealed when comparing them among themselves and with the normalized contents of elements in average compositions of picrites, Norilsk ore-bearing rocks, and continental tholeiites. The configuration of the trends characterizing the rocks of layered complexes of the western slope of the Southern Urals is very similar, differing only quantitatively (Fig.2, *e*). They are characterized by "peak" values of Ir, Rh, and Pd. The differences are in higher Cu in the Misaelga complex and a sharply reduced amount of Ni in rocks of the Kusin-Kopan complex. In the latter case, the minimum value because we are dealing only with the upper part of the intrusion, and the ultrabasic part, the existence of which was assumed earlier [2], remains inaccessible for study.

Indicator ratios of noble metals, on the one hand, are subject to significant fluctuations, on the other hand, emphasize the similarity and differences of rocks of the complexes. Thus, the average Pt_n/Pd_n in rocks of the Misaelga complex is 0.42, Pd_n/Ir_n – 7.61, $\sum EPG_n/Au_n$ – 1.72; Kusin-Kopan complex – 0.52, 2.73, 1.63, respectively; Shuidinsky complex – 0.23, 13.89, 4.32. As can be seen from the above values, the greatest similarity is characteristic of rocks of the Misaelga and Kusin-Kopan complexes.

It is evident from the diagram (Fig.2, *e*) that the configuration of the plots characterizing the rocks of layered complexes differs sharply from the plots of the "reference" rocks. To explain this situation, the diagram of normalized Ni, Cu, and noble metals distribution in sulphides from iron-enriched horizons of Norilsk deposits (Fig.2, *f*) is given. Comparative analysis of the diagrams allows us to say with high confidence that noble metals in rocks of the described complexes are concentrated in sulphides, and the question of their mineral form at the given stage of investigations remains open.

Ore mineralization of the Kusin-Kopan complex has been studied within Kopan and Matkala massifs both in natural outcrops (samples K-20, K-343, K-348) and from core samples (samples K-177, K-204). It is a vein-disseminated type with variable thickness of individual veins and ore zones. Massive ore varieties are recorded in the central parts of veins (Fig. 3, *a*), and the veins themselves have gradual contact with ore-bearing rocks. As a rule, the matrix is represented by biotite-chlorite-amphibole aggregate with a variable number of constituent minerals. The ores have an ilmenite-titaniferous magnetite composition.

All minerals are inhomogeneous on a micro-scale and represent products of multistage decomposition of the Fe-Ti-O system. Within the titaniferous magnetite crystals, thin blades, lamellae, and fabric intergrowth of titaniferous magnetite, magnetite, ulvöspinel, and hercynite, forming a complex internal pattern of multistage decomposition of solid solution, are common. Often, elongated-chain precipitates of hercynite are fixed at the boundary of ilmenite and titaniferous magnetite grains, and complex branching micro veinlets of magnetite are observed in the crystals (Fig.3, *c*). The chemical composition of titaniferous magnetite is given in Table 1.

Ilmenite is composed of xenomorphic grains and variously shaped aggregates with titaniferous magnetite crystals of various sizes (Fig.3, *b*). In most cases, ilmenite grains are homogeneous, but in some cases, parallel-located magnetite micro lamellas are present. The chemical composition of ilmenite within one orebody is stable. At the same time, differences in the ilmenite chemical composition from different objects are significant. In particular, MgO is established only in ilmenites of the Kopan massif, while an increased amount of MnO is typical for ilmenites of the Matkala massif (Table 2).

Titaniferous magnetite in massive ores and central parts of veins is represented by coalesced xenomorphic precipitates of different sizes (Fig.3, *a*, *b*). The shape of individual crystals in disseminated ores varies from xenomorphic to idiomorphic cubic-octahedral.

Ti-Fe-Cr mineralization of the Misaelga complex is established in all rock varieties. The maximum amount of Ti-Fe minerals is recorded in the upper part of the gabbro horizon, where rocks with elements

Journal of Mining Institute. 2022. Vol. 255. P. 476-492
DOI: 10.31897/PMI.2022.54

of sideronite structures are observed. The morphogenetic types of Fe and Ti oxides are variable and represented by chemically homogeneous droplet-like segregations of chrommagnetite and ilmenite. In addition, weakly faceted, prismatic, and xenomorphic precipitations of ilmenite and magnetite crystals of the octahedral form (Fig.3, *d-f*) are also recorded. A variety of ilmenite-magnetite intergrowths and decay structures with varying numbers of differently sized blades coexisting phases are often present. In titaniferous magnetite crystals, thin blades and lamellae of ilmenite (ulvöspinel) and magnetite oriented along the octahedral directions are fixed. The ilmenite lattice, which inherits the crystallographic forms of the pre-existing mineral, is retained in extreme alteration.

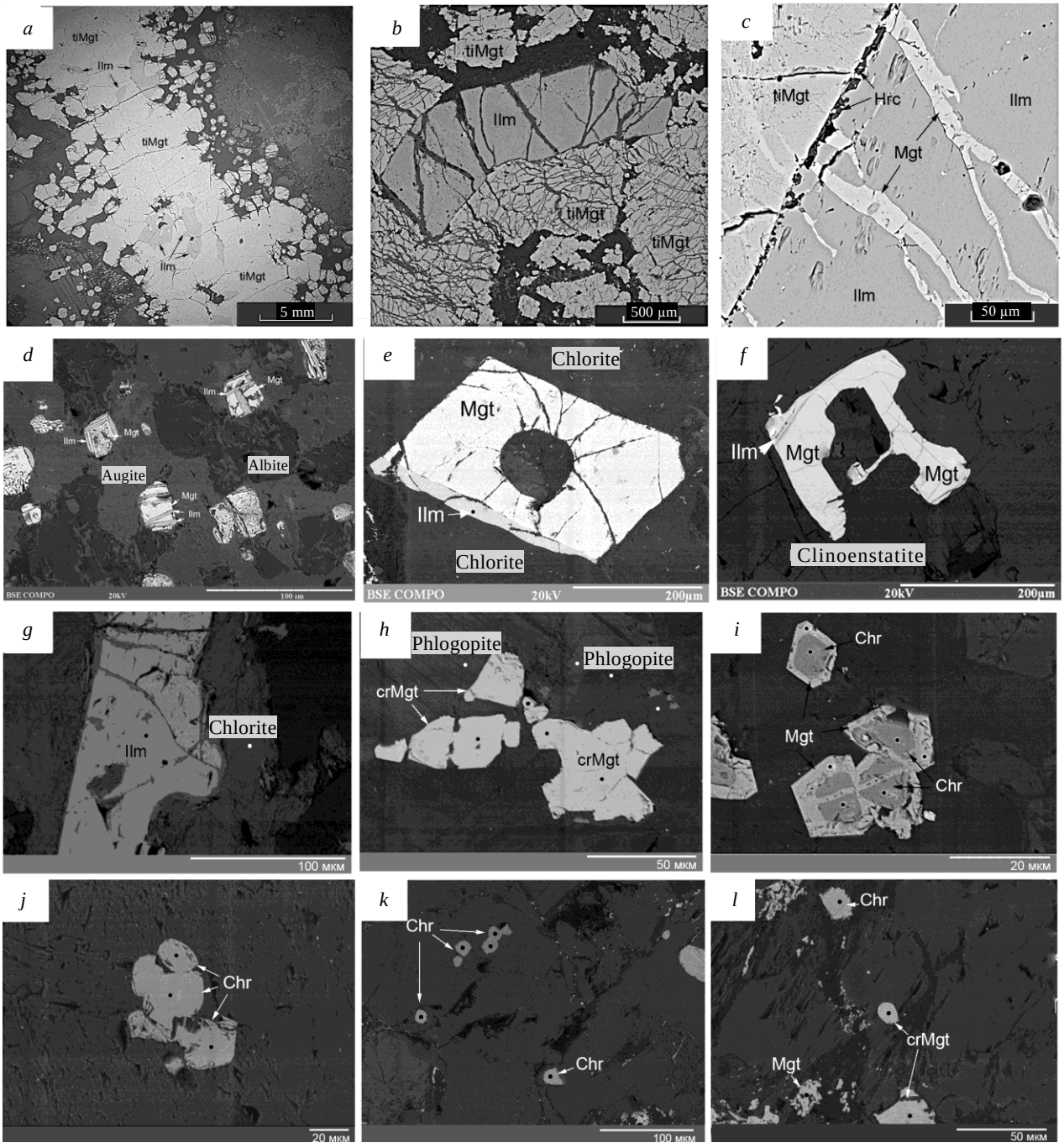

Figure 3. Morphogenetic types of Ti-Fe-Cr minerals in rocks of layered (stratified) complexes of the western slope of the Southern Urals

Complexes: *a-c* – Kusin-Kopan; *d-f* – Misaelga, *g-i* – Shuidinsky, *j-l* – Borehole N 7;
Ilm – ilmenite; tiMgt – titaniferous magnetite; Mgt – magnetite; Hrc – hercynite; Chr – chromite; crMgt – chrommagnetite

DOI: 10.31897/PMI.2022.54

Journal of Mining Institute. 2022. Vol. 255. P. 476-492

Table 1

Chemical composition of titaniferous magnetite and magnetite from rocks of the Kusin-Kopan complex, wt.%

Sample number	TiO_2	Al_2O_3	FeO	MnO	MgO	V_2O_5	Cr_2O_3	Total
K20_2	15.19	3.8	77.59	0.32	1.03	1.09	0.58	99.59
K20_3	14.03	4.9	74.21	0.31	1.34	1.02	0.6	96.41
K20_4	13.82	2.69	80.97	–	0.95	1.13	0.9	100.45
K177_8	13.71	–	85.69	0.31	–	1.33	–	101.03
K177_19	19.24	0.23	79.46	0.48	–	1.12	–	100.53
K177_23	14.62	–	81.64		–	1.09	–	97.35
K177_24	13.44	–	82.88	0.39	–	1.1	–	97.81
K204_6	7.73	1.26	86.67	–	–	1.14	0.51	97.31
K204_12	7.01	2.09	89.46	–	–	1.42	–	99.98
K204_42	8.55	–	85.73	0.2	–	1.18	–	95.66
K204_43	10.97	–	83.29	–	0.22	1.17	–	95.65
K204_44	8.96	–	86.41	–	0.21	1.17	–	96.75
K343_32	0.95	–	96.25	–	–	1.22	–	98.42
K343_33	11.06	–	87.13	0.45	–	1.15	–	99.79
K343_34	0.35	–	95.05	–	–	1.25	–	96.65
K343_35	3.92	–	92.35	–	–	1.26	–	97.53
K343_52	12.02	–	82.53	0.49	–	0.88	–	95.93
K343_68	11.54	–	81.76	0.5	–	1.07	–	94.87
K343_69	18.57	0.18	76.29	0.73	–	0.91	–	96.68
K348_14	17.53	–	77.05	0.62	–	0.98	–	96.47

Note. Hereinafter a dash means the element content is below the detection limit.

Table 2

Chemical composition of ilmenite from rocks of the Kusin-Kopan complex, wt.%

Sample number	TiO_2	FeO	MnO	MgO	Total
K204_1	51.66	47.44	1.25	–	100.35
K204_7	51.24	48.05	1.46	–	100.75
K20_6	50.1	47.96	1.0	1.2	100.26
K20_7	49.89	47.41	0.92	1.15	99.37
K20_8	51.05	47.94	0.85	1.11	100.95
K20_9	52.81	45.21	1.06	1.3	100.38
K20_13	52.08	44.21	0.83	1.19	98.31
K20_14	54.84	43.34	0.99	1.49	100.66
K20_19	55.21	42.5	1.1	1.17	99.98
K20_20	55.15	42.89	0.96	1.19	100.19
K20_27	51.13	45.15	1.05	1.23	98.56
K20_33	55.55	43.44	1.15	1.39	101.53
K20_34	55.09	43.89	1.11	1.36	101.45
K20_35	56.13	43.25	1.02	1.32	101.72
K20_47	55.29	43.62	1.1	1.45	101.46
K20_48	55.75	43.6	1.1	1.31	101.76
K177_1	52.27	46.58	1.17	–	100.02
K177_4	56.38	42.83	1.35	–	100.56
K177_5	56.56	42.21	1.25	–	100.02
K177_7	49.21	45.11	1.25	0.92	98.51
K343_30	51.54	45.41	2.05	–	99.0
K343_31	51.9	45.84	2.15	–	99.89
K343_38	51.74	46.98	2.14	–	100.86
K343_47	50.79	46.11	1.76	–	98.66
K343_48	52.48	47.53	1.95	–	101.96
K343_49	52.28	45.53	1.89	–	100.33
K343_54	49.55	48.79	1.97	–	100.32
K343_55	52.89	46.76	2.07	–	101.73
K343_56	53.74	45.41	2.09	–	101.24
K343_57	53.36	45.94	2.09	–	101.39

Journal of Mining Institute. 2022. Vol. 255. P. 476-492
DOI: 10.31897/PMI.2022.54

The chemical composition of magnetite is as follows (wt.%): titanium (0.13 to 14.27), aluminium (0.51 to 21.36), chromium (0.48 to 24.07), magnesium (0.11 to 6.41), manganese (0.05 to 1.0), vanadium (0.23 to 1.16), and zinc (0.8 to 5.78), nickel (0.13 to 0.73), silica (0.52 to 2.75), and calcium (0.51). The content of trace components in ilmenites varies in the following ranges (wt.%): chromium (0.13 to 1.27), magnesium (0.27 to 5.5), manganese (0.14 to 3.51), vanadium (0.14 to 0.37) as well as aluminium (3.0), and nickel (1.4) [14].

A detailed study of the mineralization reveals a very regular distribution of trace elements depending on the location of the mineral in the intrusive body section, which is the result of melt differentiation in the intermediate chamber. In particular, chromium and magnesium in magnetite and ilmenite are presented only in minerals of the ultrabasic horizon, where, as a result of heterovalent isomorphism, transitional varieties magnetite → chrommagnetite and ilmenite → picroilmenite are formed. The distribution of vanadium in magnetite is relatively stable, and the maximum amount of manganese is found in ilmenite of the ultramafic horizon, where it most likely isomorphically replaces the MgO and Cr_2O_3 positions.

Ti-Fe-Cr mineralization of the Shuidinsky complex is also widespread throughout the intrusive body. In the gabbro horizon, the mineralization is represented by magnetite, titaniferous magnetite, and ilmenite, both individually and forming various intergrowths (Fig.3, *g*). Due to the significant degree of metamorphism in the complex, magnetite often occurs as a product of sulphide substitution. In this case, CuO, CoO, NiO, and S are fixed in their composition. The composition of titaniferous magnetite and ilmenite from the gabbro horizon is rather stable (Table 3).

In the Ti-Fe-Cr ultrabasic horizon, the mineralization is more diverse. Magnetite, chrommagnetite, chromite, and ilmenite are found here. Magnetite occurs as individual octahedral crystals and in intergrowth with chromspinels, but more often forms metamorphogenic rims around the latter (Fig.3, *i*). Chrommagnetite is established in the upper parts of the ultrabasic horizon as crystals of octahedral and cubic forms, often forming monomineral intergrowths (Fig.3, *h*). The chromspinels are widespread throughout the ultramafic horizon as individual crystals of octahedral and truncated-octahedral forms. The crystals often form various intergrowths and are surrounded by magnetite and chrommagnetite rims. Their chemical composition is given in Table 4.

Table 3

Chemical composition of Ti-Fe-Cr minerals from rocks of the Shuidinsky complex, wt.%

N	Sample number	SiO_2	TiO_2	Al_2O_3	V_2O_5	Cr_2O_3	FeO	MnO	MgO	Total
1	15799	–	48.27	–	–	–	46.19	4.68	–	99.14
2	15799	–	48.48	–	–	–	45.99	4.6	–	99.07
3	15799	–	48.4	–	–	–	45.99	4.73	–	99.12
4	15799	–	48.51	–	–	–	45.84	4.76	–	99.11
5	15799	–	49.97	–	–	–	43.38	5.8	–	99.15
6	15799	–	49.13	–	–	–	43.57	6.3	–	99.0
7	15799	–	48.51	–	–	–	45.84	4.76	–	99.11
8	15808	–	48.81	–	–	–	48.14	2.22	–	99.17
9	15808	–	48.66	–	–	–	48.02	2.5	–	99.18
10	15808	–	48.75	–	–	–	47.75	2.53	–	99.59
11	15811	–	50.63	–	–	–	45.3	3.66	–	99.03
12	15812	–	50.1	–	–	–	45.5	3.56	–	99.16
13	k-278	–	0.91	21.92	–	35.18	30.33	–	10.73	99.07
14	k-278	–	0.87	23.18	–	34.43	29.57	–	11.11	99.16
15	k-278	–	1.56	20.51	–	32.37	33.88	–	10.69	99.01
16	k-353	1.27	0.76	11.33	0.43	33.64	43.28	0.23	5.96	96.9
17	k-353	–	0.62	12.87	0.48	37.72	41.11	0.17	6.39	99.36
18	k-353	0.69	0.56	13.43	0.4	37.71	40.17	0.05	6.27	99.28
19	k-353	0.75	0.56	13.5	0.47	37.27	39.84	0.13	6.73	99.25
20	k-353	0.64	0.59	13.63	0.45	37.54	39.87	0.17	6.4	99.29

Note. 1-12 – gabbro; 13-20 – ultrabasic horizon.

DOI: 10.31897/PMI.2022.54

Journal of Mining Institute. 2022. Vol. 255. P. 476-492

Table 4

Chemical composition of Ti-Fe-Cr minerals from rocks of the Borehole N 7, wt.%

N	Sample number	TiO_2	Al_2O_3	Cr_2O_3	V_2O_5	FeO	MnO	MgO	ZnO	Total
1	27120b	0.44	–	6.29	0.6	85.62	–	–	–	92.96
2	27120c	0.52	1.22	8.64	0.66	82.77	–	0.14	–	93.96
3	7_49	2.47	1.53	10.85	1.08	75.99	0.42	0.37	0.45	93.15
4	7_49	6.85	2.67	36.96	0.32	47.68	0.48	1.37	0.80	97.14
5	7_49	5.05	3.37	22.74	0.66	61.62	0.73	0.83	0.83	95.82
6	7_49	8.39	1.26	41.62	0.35	43.75	0.00	2.07	0.47	97.92
7	7_49	7.89	5.05	26.45	0.73	54.59	0.83	1.45	0.64	97.62
8	7_49	7.09	2.32	32.42	0.65	52.62	0.59	1.36	0.73	97.79
9	7_49	7.34	2.40	30.45	–	52.74	0.64	1.13	1.09	95.80
10	7_38.5	–	30.27	21.77	1.62	32.77	0.00	12.94	–	99.36
11	7_38.5	–	24.38	23.76	1.97	36.36	0.45	11.24	–	98.15
12	7_38.5	–	23.85	27.97	1.58	33.44	0.00	11.51	–	98.36
13	7_38.5	–	29.92	20.25	1.82	34.64	0.39	13.00	–	100.02
14	7_38.5	–	28.11	22.45	1.75	33.49	0.00	12.57	–	98.37
15	7_38.5	0.23	26.22	23.52	1.76	34.64	0.64	12.39	–	99.40
16	27120a	0.55	3.42	20.49	0.76	68.18	–	0.17	0.71	94.28
17	27121a	–	17.02	39.67	0.48	38.27	0.13	2.23	1.25	99.04
18	27121b	–	16.45	43.72	0.61	31.07	0.17	7.02	0.18	99.22
19	27121c	–	16.73	44.79	0.42	27.1	0.04	10.02	0.12	99.22
20	27123a	0.48	17.62	38.28	0.12	39.31	0.43	0.96	1.94	99.15
21	27123c	–	17.09	37.55	0.6	41.26	0.26	0.39	1.97	99.11
22	27123d	–	16.44	37.86	0.52	41.12	0.56	0.48	2.19	99.18
23	27123e	–	15.83	37.44	0.66	42.28	0.45	0.54	1.99	99.17
24	7_49	–	52.48	0.31	0.00	44.69	1.19	1.72	–	100.38
25	7_38.5	–	–	–	15.20	67.38	–	–	–	82.58
26	7_38.5	–	–	–	19.14	73.14	–	–	–	92.27

Note. 1-3 – chrommagnetite; 4-23 – chromspinel; 24 – hercynite; 25, 26 – unidentified compounds.

Ti-Fe-Cr mineralization in rocks drilled in the Borehole N 7 is represented by magnetite, chrommagnetite, and chromspinel (Fig.3, *j-l*). Magnetite occurs throughout the whole ore body, usually as xenomorphic aggregates and submicron segregations tracing cracks in olivine.

Chrommagnetite is more abundant in the upper part of the ore body, where they are arranged as octahedral crystals, often with rounded edges, and xenomorphic aggregates are located either inside clinopyroxene crystals or in the interstitial space (Fig.3, *j*). The most frequent mineral is chromspinel, which is widespread throughout the section as well-cut octahedral crystals, rounded, less frequently xenomorphic forms. It is observed as small (first microns) crystals poikilitically included in olivine and clinopyroxene grains, and also occurs in separate crystals or glomerocrystalline aggregates and intergrowths (Fig.3, *j-l*). The chemical composition of the minerals is given in Table 4. In addition, the rocks contain hercynite and unidentified iron-vanadium compounds, which are most likely intermediate members of the series magnetite ($FeO{\cdot}Fe_2O_3$) – shubnelite ($FeVO_4$) H_2O – coulsonite (FeV_2O_4).

Classification diagrams (Fig.4) reveal features of Ti-Fe-Cr mineralization inherent to individual massifs, and general trends characterizing mineralization during its formation. Thus, in the Al-Cr-Fe^{3+}+2Ti diagram (Fig.4, *a*) the change in oxides compositions is caused by melt differentiation. In particular, in the Shuidinsky complex, mineral variations correspond to chromspinel-chrommagnetite compound; in rocks of the Borehole N 7 – to aluminian chromite-ferrichromite-chrommagnetite; in Misaelga complex – to chrommagnetite-magnetite and in Kusin-Kopan complex – to magnetite.

On the diagram by S.J.Barnes and P.L.Rodger [22] (Fig.4, *b*) the figurative points of Ti-Fe-Cr oxides of practically all complexes fall into the field of stratified intrusions, that in general is an indicator of the commonality of differentiation processes despite the differences in crystallization conditions of Ti-Fe-Cr minerals, typical to different world complexes.

Journal of Mining Institute. 2022. Vol. 255. P. 476-492
DOI: 10.31897/PMI.2022.54

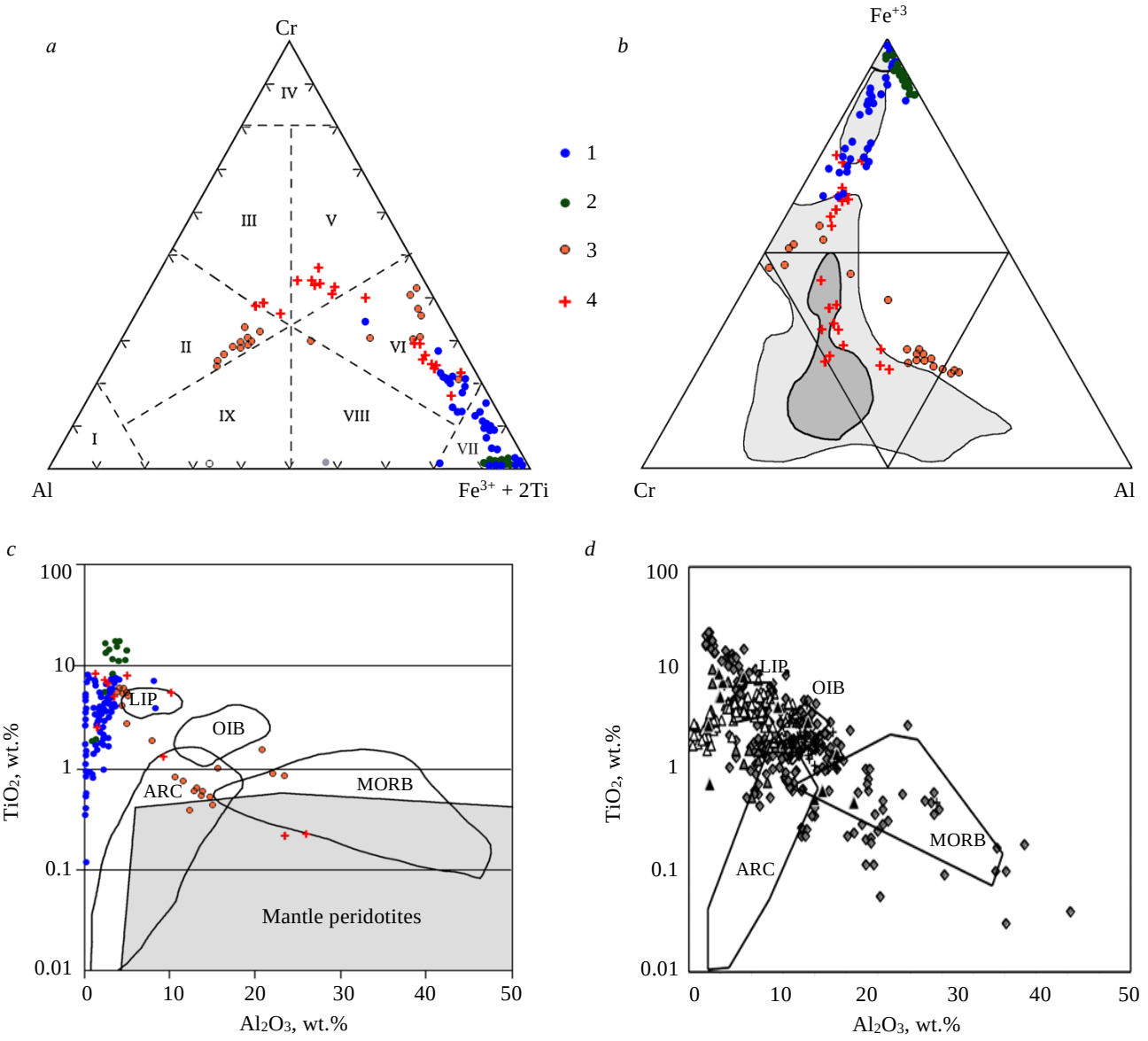

Fig.4. Classification diagrams for Ti-Fe-Cr minerals from rocks of layered (stratified) complexes of the western slope of the Southern Urals

Diagrams: *a* according to [23]: I – spinel; II – chromium spinel; III – aluminian chromite; IV – chromite; V – ferrichromite; VI – chrommagnetite; VII – magnetite; VIII – aluminian magnetite; IX – hercynite; *b* according to [22] the fields of layered intrusions are marked; *c* according to [24] the fields are marked: LIP – large magmatic provinces; OIB – ocean island basalts; ARC – island-arc basalts; MORB – mid-ocean ridge basalts; *d* according to [25] for Ti-Fe-Cr minerals of Siberian traps, Karru dolerites and Deccan traps; 1 and 2 – Misaelga and Kusin-Kopan complexes; 3 – rocks of Borehole N 7; 4 – Shuidinsky complex

Earlier studies have established that the TiO_2 content in chromspinel can be a reliable indicator of magma composition and as a consequence characterize the geotectonic setting of their formation [24, 26-28]. Diagram TiO_2-Al_2O_3 (Fig.4, *c*) shows, that figurative points of mineral compositions from the layered complexes of the western slope of the Southern Urals are grouped outside the boundaries of selected fields. Moreover, the chromspinels of the Shuidinsky complex and from the Borehole N 7 rocks form a clear trend illustrating an inverse relationship between Ti and Al content in their composition, if the points are haphazardly arranged relative to the separated fields. That is, the existing dependencies between TiO_2 and Al_2O_3 in the composition of Ti-Fe-Cr minerals are more diverse and complex than the fields highlighted in the diagram. It should be noted that the chromspinels of Siberian traps, Karru dolerites, and Deccan traps also do not fit into the fields allocated on the diagram TiO_2-Al_2O_3 (Fig.4, *d*) [25].

DOI: 10.31897/PMI.2022.54

Journal of Mining Institute. 2022. Vol. 255. P. 476-492

Comparative analysis of the main components in magnetite from layered complexes revealed interesting regularities (Fig.5). They are summarised as follows:

• to check the correctness of the author's data on the Kusin-Kopan complex (Kopan and Matkala massifs) the Ti-Fe mineralization of the Medvedev massif by V.V.Kholodnov et al. [3] was added to the diagrams. The points characterizing the distribution of components in magnetites of the Kopan, Matkala, and Medvedev massifs form uniform fields in all the diagrams (Fig.5);

• The FeO-Cr_2O_3 diagram shows a clear inverse relationship between the components in magnetites of the Shuidinsky complex and the Borehole N 7. At the same time, the trend characterizing magnetites of Misaelga complex in the area ~ FeO – 85 %, Cr_2O_3 – 1 % is bifurcated so that one branch is on the general trend for layered bodies, and the second one corresponds to content variations in magnetites of Kusin-Kopan complex. While preserving the general trends inherent to the layered complexes, the behavior of Cr_2O_3 in magnetites of the gabbro horizon of the Misaelga intrusion and ore objects of the Kusin-Kopan complexes are identical;

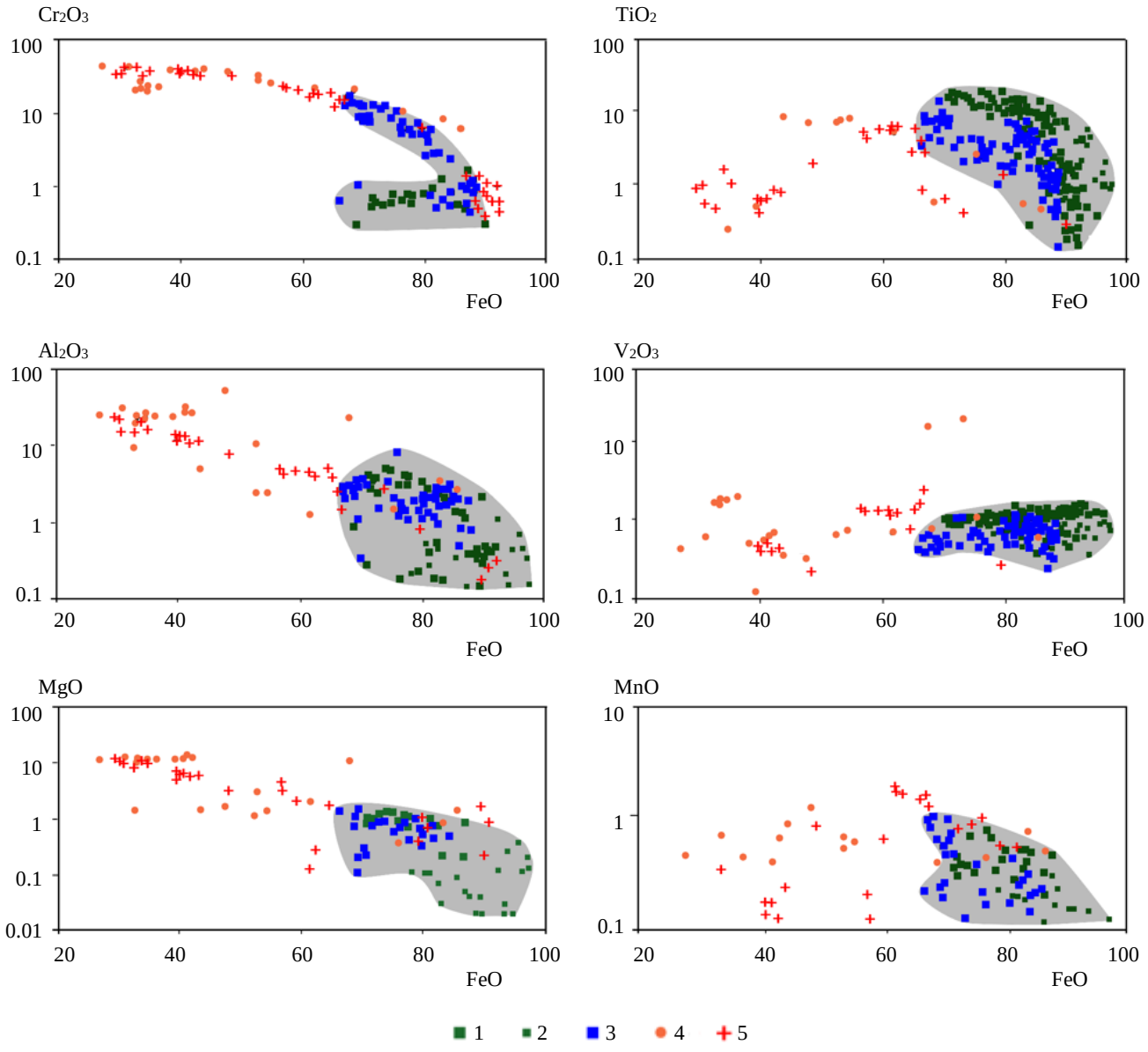

Fig.5. Chemical composition of magnetite from layered complexes of the western slope of the Southern Urals

1 – Kopan and Matkala massifs of the Kusin-Kopan complex; 2 – Medvedev massif of the Kusin-Kopan complex according to [3]; 3 – Misaelga complex; 4 – rocks of the Borehole N 7; 5 – Shuidinsky complex

Journal of Mining Institute. 2022. Vol. 255. P. 476-492
DOI: 10.31897/PMI.2022.54

• FeO-MgO and FeO-Al_2O_3 diagrams of all the complexes fit in a single trend characterizing the behaviour of MgO and Al_2O_3 during melt differentiation, but the magnetites of the Misaelga and Kusin-Kopan complexes are located in the "ferrous" and "low alumina" part of the trend, while the points of magnetites from the Shuidinsky complex and rocks of the Borehole N 7 – in the "magnesian" and "high alumina";

• in the diagrams FeO-TiO_2, FeO-V_2O_3, and FeO-MnO magnetites of Misaelga and Kusin-Kopan complexes form unified fields, whereas the distribution of these components in magnetites of the Shuidinsky complex and rocks of the Borehole N 7 are haphazard.

Thus, the analysis of the chemical composition of magnetite from layered complexes showed significant similarity of mineralization of the Misaelga and Kusins-Kopan complexes in almost all parameters, which may serve as evidence of the similarity of its formation mechanisms.

Formation and transformation conditions of Fe-Ti-Cr mineralization can be obtained by calculation methods as well as by analysing the chemical composition of the accompanying minerals. It follows from the location of figurative points on the diagram lgfO_2-T, °C (Fig.6, *a*) that the crystallization temperature of magnetite-ilmenite aggregates from rocks of the Misaelga complex varies within 712-745 °C. The variation interval for 12 samples is 648-745 °C. The temperature of solid solution decomposition calculated for 15 samples is 588-766 °C. As can be seen from the diagram lgfO_2-*T*, °C (see Fig.6, *a*), the partial pressure of O_2 during crystallization of the melt decreased with decreasing temperature, indicating that the system is closed towards oxygen and relatively weak oxidation of the melt (points are located below the hematite-magnetite stability locus). The equilibrium temperature of coexisting Fe-Ti phases in metamorphic rocks of the Shuidinsky complex reaches 645-792 °C, and the oxygen fugacity varies from –17 to –14.7. At the same time, a part of points falls into the field limited by the NNO-QFM locus. That is, during the formation of Fe-Ti minerals and their transformation during metamorphism, the partial pressure of oxygen decreased. The figurative points calculated for the Fe-Ti minerals from rocks of the Kusin-Kopan complex are grouped into two fields (Fig.6, *a*), the first of which (*T* = 635-822°C, lgfO_2 = –18.8-14.6) corresponds to the magmatic stage of mineral formation, and the second (*T* = 483-606° C, lgfO_2 from –24.2 to –21.7) corresponds to the metamorphogenic re-equilibration of the system.

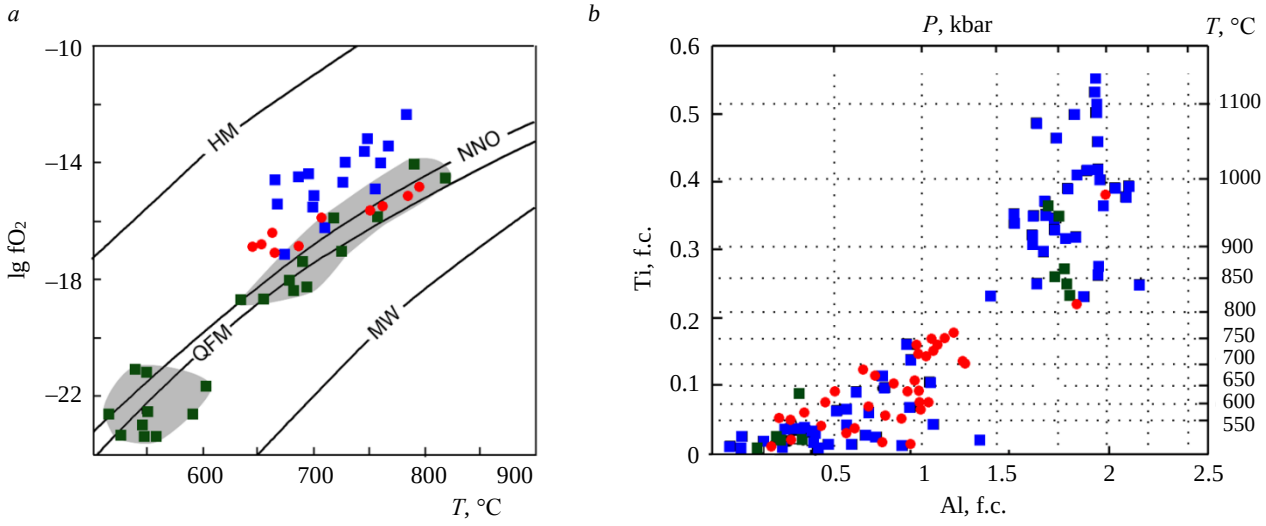

Fig.6. Diagrams lgfO_2-T, °C for Fe-Ti minerals and Ti (f.c.)-Al (f.c.) for amphiboles from rocks of layered (stratified) complexes of the western slope of the Southern Urals

1 – Kusin-Kopan, 2 – Misaelga, 3 – Shuidinsky complexes.
Stability locus HM and MW by [29], QFM by [30], NNO by [31]. Grey fill *a* – fields of the Kusin-Kopan complex

To estimate *P-T* metamorphism parameters, the diagram Ti (f.c.)-Al (f.c.) [32-34] was constructed for amphiboles from rocks of layered complexes (Fig. 6, *b*). It is noteworthy that the points characterizing amphiboles of all complexes are clustered in two fields with a well-registered temperature boundary of 800 °C, separating primary magmatic amphibole from metamorphic amphibole. Thus, metamorphism parameters, which caused component redistribution in Fe-Ti-Cr minerals of layered complexes, are as follows: Misaelga – T = <550-750 °C, P = 0.1-2.8 kbar; Kusin-Kopan – T = <550-630 °C, P = 0.3-0.7 kbar, and Shuidinsky complexes – T = <550-760 °C, P = 0.5-2.5 kbar.

The above detailed geochemical analysis of rocks composing layered bodies and characteristics of Ti-Fe-Cr mineralization showed that there is a similarity of REE redistribution processes in rocks of Misaelga and Kusin-Kopan complexes; by indicator relations of noble metals the greatest similarity is also typical for rocks of Misaelga and Kusin-Kopan complexes; variations of the main components of the chemical composition of magnetite show the significant similarity of the Misaelga and Kusin-Kopan complexes. That facts allow us to use the intrusive body of the Misaelga complex as a "reference" object to clarify conditions and mechanisms of rock formation from the Kusin-Kopan complex and associated Ti-Fe-Cr mineralization.

We simulated the crystallization process using two models: by software product COMAGMAT, version 5.2.2.1 [35-37] and the algorithm of H.D.Nathan and C.K.Vankirk [38]. The calculated weighted average composition of the intrusive body of the Misaelga complex (wt.%) was taken as the melt consisting SiO_2 – 48.23, TiO_2 – 1.87, Al_2O_3 – 8.4, FeO – 17.11, MnO – 0.2, MgO – 14.74, CaO – 8.32, Na_2O – 1.37, K_2O – 0.62. After obtaining the simulation results, the crystallization diagrams were plotted (Fig.7).

The fractional crystallization of the melt calculated by the software product COMAGMAT is shown in Fig.7, *a*. The first released phase at 1380° C will be Ol (77-85 % Fo), then Cpx joined at T – 1164 °C, with a result of 40 % of the melt volume being represented by a bimineral Ol + Cpx association. Further in the temperature range of 1139-904 °C Cpx + Pl + Pg + tiMgt + Ilm association is released. The remaining 10 % of the melt is interstitial material whose crystallization is not described within the framework of the given model. Crystallization of the melt according to the algorithm of H.D.Nathan and C.K.Vankirk [38] (Fig.7, *b*) begins with Ol at 1304 °C, after about 24 % crystals, tiMgt is released on the liquidus, and at 1207° C, Cpx + tiMgt association with small amount of Ol crystallizes. As a result, when the temperature decreases to 1185 °C, about 48 % of the melt volume is represented by Ol + Cpx + tiMgt association. In the temperature interval 1185-1143 °C Pl + Cpx + Opx + Mgt + Ol association crystallizes in the proportions shown in the diagram (see Fig.7, *b*). The melt composition in this interval is probably close to eutectic, which is shown in the diagram as alternating bands representing crystallization from the melt of one of the minerals. Then Pl + Opx + Cpx + tiMgt association crystallizes, followed by Or + Pl + Q, which completes the process of the intrusive body formation. Analysis of the diagram indicates that its upper part fully corresponds to the real structure of the stratified part of the Kusin-Kopan complex. It should be emphasized in both cases that the complex should have an ultrabasic horizon, represented by Ol + Cpx rocks.

Earlier, during the detailed study of the Kusin-Kopan complex it was established that "... based on the geochemical comparison of the marginal group rocks and horizon of ilmenite gabbro-norites, it is reasonable to conclude that in the section of the stratified series there is a complex unexplored zones or horizons of magnesian rocks close to peridotites, pyroxenites and their plagioclase varieties... Undoubtedly, the large volumes of high-density ultrabasic and basic rocks among predominantly metasedimentary formations should be reflected in the geophysical fields. A large and enigmatic positive area (up to 20×30 km) gravity anomaly in this area of the Urals is located 10-20 km east of the

Journal of Mining Institute. 2022. Vol. 255. P. 476-492
DOI: 10.31897/PMI.2022.54

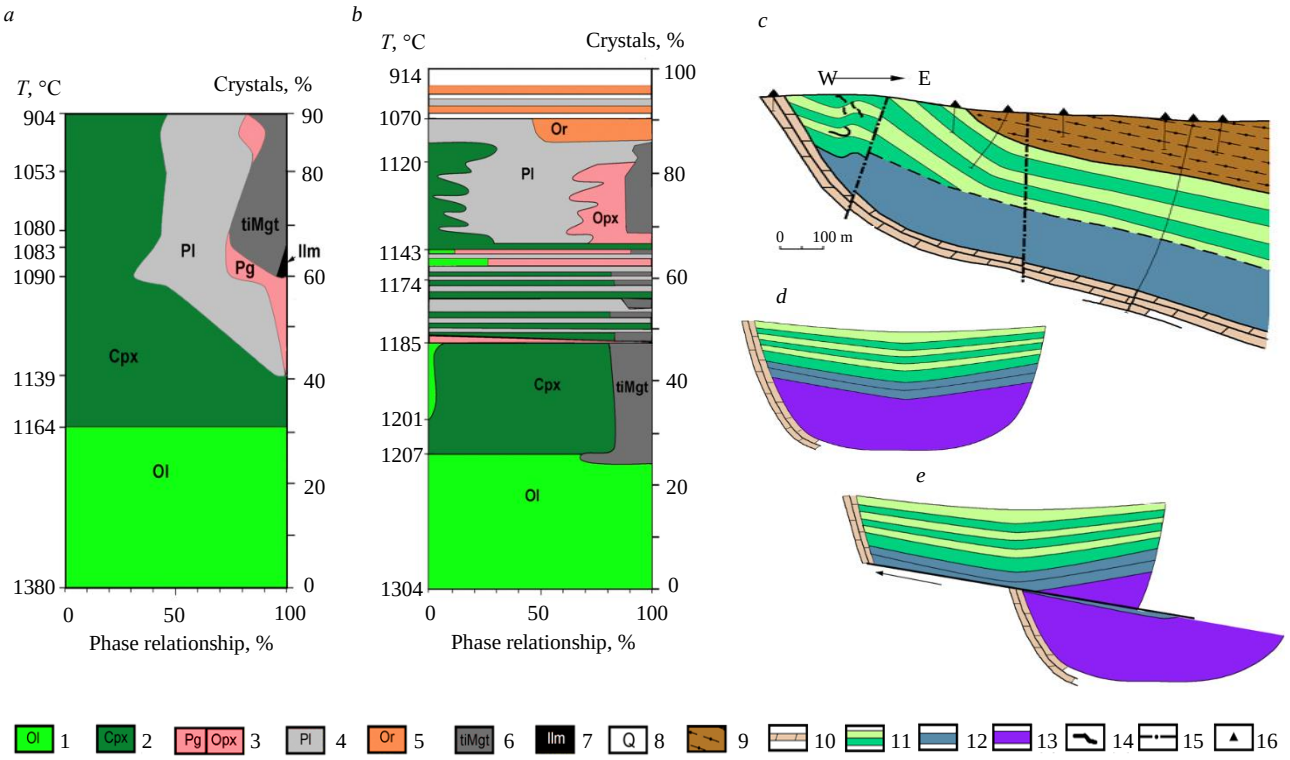

Fig.7. Crystallization diagrams of the average weighted composition from the Misaelga complex according to the software product COMAGMAT (*a*) and the algorithm of H.D.Nathan and C.K.Vankirk [38] (*b*), geological section of the uncovered part of the Kusin massif according to [2], with modifications (*c*) and idealized cross-section of the Kusin-Kopan complex (*d*, *e*)

1 – olivine; 2 – clinopyroxene; 3 – orthopyroxene; 4 – plagioclase; 5 – orthoclase; 6 – titaniferous magnetite; 7 – ilmenite; 8 – quartz; 9 – biotite-amphibole gneisses of the Kuvashi suite; 10 – carbonate rocks, Satka suite (R_1); 11 – stratified zone; 12 – gabbro-norite zone with ilmenite; 13 – inferred horizon of ultrabasic rocks; 14 – spent ilmenite-magnetite ores; 15 – tectonic disturbances; 16 – exploration boreholes. Ol – olivine; Cpx – clinopyroxene; Opx – orthopyroxene; Pl – plagioclase; Or – orthoclase; Mgt – magnetite; tiMgt – titanomagnetite; Q – quartz

band of surface-mapped intrusions of the complex in the latitude of the southern part of the Kopan massif with a maximum near the Lake Semibratskoe. We have no doubt that this anomaly is caused by a still unexplored part of a very large stratified intrusion" [2, p. 96].

Thus, modelling of the melt crystallisation process indicates that the Kusin-Kopan complex should represent a loppolyte-like body, which idealized cross-section is shown in Fig.7, *d*. As a result of collisional processes that occurred in the area in the Vendian and/or Late Palaeozoic [39] time, the lower ultrabasic part of the intrusion has been detached from the upper part (Fig.7, *e*). The fact that the boundary between the basic and ultrabasic horizons of layered intrusions is a "weakened" zone is fixed by the example of the Misaelga complex, where despite relatively weak metamorphism, rocks of the transition zone are completely metamorphic and contain garnet (grossular) + amphibole + epidote + chlorite mineral association.

The proposed structure of the Kusin-Kopan complex sharply increases its prospects for minerals such as platinum group minerals + sulphide copper-nickel minerals and/or chromites, because elements of the platinum group, nickel sulphides, and chromite mineralization are concentrated in the lower (ultramafic) horizon of the layered body, as we have shown earlier on the example of the Misaelga complex [14].

Conclusions. The detailed geochemical analysis of the rocks composing the layered (stratified) bodies of the western slope of the Southern Urals and characteristics of Ti-Fe-Cr mineralization showed similarity of REE redistribution processes in rocks of the Misaelga and Kusin-Kopan com-

plexes. In addition, in terms of indicator ratios of noble metals, the greatest similarity is also characteristic of the rocks of the Misaelga and Kusin-Kopan complexes, and variations in the chemical composition of magnetites indicate a significant mineralization similarity for both these complexes in almost all parameters.

It was established that metamorphism causing component redistribution in Fe-Ti-Cr minerals of layered complexes, corresponds to the following parameters: Misaelga – T = <550-750 °C, P = 0.1-2.8 kbar, Kusin-Kopan – T = <550-630 °C, P = 0.3-0.7 kbar and Shuidinsky complexes – T = <550-760 °C, P = 0.5-2.5 kbar.

As a result of melt crystallization modelling, it is shown that the Kusin-Kopan complex is an intrusive body with an ultramafic horizon in an idealized cross-section. Because of collisional processes, the lower part of the intrusion has been detached from the upper part. The proposed structure of the Kusin-Kopan complex dramatically increases its prospects for minerals such as platinum group minerals + sulphide copper-nickel minerals and/or chromites.

REFERENCES

1. Smirnov V.I. Ore Deposits of the USSR. In 3 volumes. Vol. 2. Moscow: Nedra, 1978, p. 352 (in Russian).

2. Alekseev A.A., Alekseeva G.V., Kovalev S.G. Stratified intrusions of the western slope of the Urals. Ufa: Gilem, 2000, p. 188 (in Russian).

3. Holodnov V.V., Bocharnikova T.D., Shagalov E.S. Structure, age and genesis of magnetite-ilmenite ores of the Middle Riphean stratified Medvedevskii massif (Kusinsko-Kopanskii complex of Southern Ural). *Lithosphere* (*Russia*). 2012. N 5, p. 145-165 (in Russian).

4. Alekseev A.A., Alekseeva G.V., Kovalev S.G. Layered intrusions of the western slope of the Urals. Ufa: Gilem, 2003, p. 171 (in Russian).

5. Mazurov M.P., Vasilev Y., Shikhova A.V., Titov A.T. Assemblages and Structure of Ore Minerals in Intrusive Traps of the Western Part of the Siberian Platform. *Russian Geology and Geophysics*. 2014. Vol. 55. N 1, p. 78-88 (in Russian). DOI: 10.1016/j.rgg.2013.12.006

6. Zhong-Jie Bai, Hong Zhong, Anthony J. Naldrett et al. Whole-rock and mineral composition of constraints on the genesis of the giant Hongge Fe-Ti-V oxide deposit in the Emeishan Large Igneous Province, Southwest China. *Economic Geology*. 2012. Vol. 107. N 3, p. 507-524. DOI: 10.2113/econgeo.107.3.507

7. Kwan-Nang Pang, Mei-Fu Zhou, Donald Lindsley et al. Origin of Fe-Ti oxide ores in mafic intrusions: evidence from the Panzhihua Intrusion, SW China. *Journal of Petrology*. 2008. Vol. 49. N 2, p. 295-313. DOI: 10.1093/petrology/egm082

8. Charlier B., Grove T.L. Experiments on liquid immiscibility along tholeiitic liquid lines of descent. *Contributions to Mineralogy and Petrology*. 2012. Vol. 164, p. 27-44. DOI: 10.1007/s00410-012-0723-y

9. Jakobsen J.K., Veksler I.V., Tegner C., Brooks C.K. Crystallization of the Skaergaard intrusion from an emulsion of immiscible iron- and silica-rich liquids: evidence from melt inclusions in plagioclase. *Journal of Petrology*. 2011. Vol. 52. Iss. 2, p. 345-373. DOI: 10.1093/petrology/egq083

10. Veksler I.V., Dorfman A.M., Borisov A.A. et al. Liquid immiscibility and the evolution of basaltic magma. *Journal of Petrology*. 2007. Vol. 48. Iss. 11, p. 2187-2210. DOI: 10.1093/petrology/egm056

11. Veksler I.V., Charlier B. Silicate Liquid Immiscibility in Layered Intrusions. Layered Intrusions. Book Chapter in Springer Geology. 2015, p. 229-258. DOI: 10.1007/978-94-017-9652-1_5

12. Wang C.Y., Zhou M.F. New textural and mineralogical constraints on the origin of Hongge Fe-Ti-V oxide deposits, SW China. *Mineralium Deposita*. 2013. Vol. 48. Iss. 6, p. 787-798. DOI: 10.1007/s00126-013-0457-4

13. Sharkov E.V., Chistyakov A.V., Bogina M.M. et al. Origin of Fe-Ti Oxide Mineralization in the Middle Paleoproterozoic Elet'ozero Syenite-Gabbro Intrusive Complex (Northern Karelia, Russia). *Geology of Ore Deposits*. 2018. Vol. 60. N 2, p. 172-200 (in Russian). DOI: 10.1134/S1075701518020046

14. Kovalev S.G., Kovalev S.S. Conditions and mechanisms of sulphide-oxide mineralization during melt differentiation in the intermediate chamber (by the example of the western slope of the Southern Urals intrusion). *Geologiya rudnykh mestorozhdenii*. 2021. Vol. 63. N 6, p. 551-575 (in Russian). DOI: 10.31857/s0016777021060034

15. Kovalev S.G., Kovalev S.S. On the melt differentiation in the intermediate chamber (by the example of differentiated intrusives of the western slope of the Southern Urals). *Georesources.* 2021. Vol. 23. Iss. 4, p. 80-95 (in Russian). DOI: 10.18599/grs.2021.4.10

16. Kovalev S.G., Snachev V.I., Romanovskaya M.A. New geological and petrogenetic aspects of Kusin-Kopan complex formation. *Vestnik Moskovskogo universiteta*. Seriya 4: Geologiya. 1995. N 4, p. 81-85 (in Russian).

17. Petrographic Code of Russia. Magmatic, metamorphic, metasomatic, impact formations. Chief editors: O.A.Bogatikov, O.V.Petrov. St. Petersburg: VSEGEI, 2008, p. 203 (in Russian).

18. Irvine T.N., Baragar W.R.A. A guide to the chemical classification of the common rocks. *Canadian Journal of Earth Sciences*. 1971. Vol. 8, p. 523-548.

19. Barnes S.J., Maier W.D. The fractionation of Ni, Cu and the noble metals in silicate and sulfide liquids. Dynamic Processes in Magmatic Ore Deposits and their application in mineral exploration. Geological Association of Canada, Short Course. 1999. Vol. 13, p. 69-106.

20. Barnes S.J., Lightfoot P.C. Formation of magmatic nickel sulfide deposits and processes affecting their copper and platinum group element contents. Book Chapter Economic geology in One Hundredth Anniversary Volume. Society of Economic Geologists, 2005, p. 179-213. DOI: 10.5382/av100.08

21. McDonough W.F., Sun S.S. The composition of the Earth. *Chemical Geology*. 1995. Vol. 120. Iss. 3-4, p. 223-253. DOI: 10.1016/0009-2541(94)00140-4

22. Barnes S.J., Roeder P.L. The Range of Spinel Compositions in Terrestrial Mafic and Ultramafic Rocks. *Journal of Petrology*. 2001. Vol. 42. Iss. 12, p. 2279-2302. DOI: 10.1093/petrology/42.12.2279

23. Okrugin A.V. Importance of Chrome Spinellid Typomorphism for Prognosis of Alluvial Platinum's Primary Sources in the Eastern Part of the Siberian Platform. *Domestic Geology*. 2005. N 5, p. 3-10 (in Russian).

24. Kamenetsky V.S., Grawford A.J., Meffre S. Factors Controlling Chemistry of Magmatic Spinel: an Empirical Study of Associated Olivine, Cr-spinel and Melt Inclusions from Primitive Rocks. *Journal of Petrology*. 2001. Vol. 42. Iss. 4, p. 655-671. DOI: 10.1093/petrology/42.4.655

25. Melluso L., de'Gennaro R., Rocco I. Compositional variations of chromiferous spinel in Mg-rich rocks of the Deccan Traps, India. *Journal of Earth System Science*. 2010. Vol. 119. Iss. 3, p. 343-363. DOI: 10.1007/s12040-010-0021-x

26. Glassley W. Geochemistry and tectonics of the Crescent volcanic rocks, Olympic Peninsula, Washington. *Geological Society of America Bulletin*. 1974. Vol. 85. N 5, p. 785-794. DOI: 10.1130/0016-7606(1974)85<785:GATOTC>2.0.CO;2

27. Arai S. Chemistry of chromian spinel in volcanic rocks a potential guide to magma chemistry. *Mineralogical Magazine*. 1992. Vol. 56. Iss. 383, p. 173-184. DOI: 10.1180/minmag.1992.056.383.04

28. Arai S., Okamura H., Kadoshima K. et al. Chemical characteristics of chromian spinel in plutonic rocks: Implications for deep magma processes and discrimination of tectonic setting. *Island Arc*. 2011. Vol. 20. Iss. 1, p. 125-137. DOI: 10.1111/j.1440-1738.2010.00747.x

29. Myers J., Eugster H.P. The system Fe-Si-O: oxygen buffer calibrations to 1,500 K. *Contributions to Mineralogy and Petrology*. 1983. Vol. 82. Iss. 1, p. 75-90. DOI: 10.1007/bf00371177

30. Berman R.G. Internally-consistent thermodynamic data for minerals in the system Na_2O-K_2O-CaO-MgO-FeO-Fe_2O_3-$A1_2O_3$-SiO_2-TiO_2-H_2O-CO_2. *Journal of Petrology*. 1988. Vol. 29. Iss. 2, p. 445-522. DOI: 10.1093/petrology/29.2.445

31. Huebner J.S., Sato M. The oxygen fugacity-temperature relationships of manganese oxide and nickel oxide buffers. *American Mineralogist*. 1970. Vol. 55. N 5-6, p. 934-952.

32. Féménias O., Mercier J.-C.C., Nkono C. et al. Calcic amphibole growth and compositions in calc-alkaline magmas: Evidence from the Motru Dike Swarm (Southern Carpathians, Romania). *American Mineralogist*. 2006. Vol. 91. N 1, p. 73-81. DOI: 10.2138/am.2006.1869

33. Mutch E.J.F., Blundy J.D., Tattitch B.C. et al. An experimental study of amphibole stability in low-pressure granitic magmas and a revised Al-in-hornblende geobarometer. *Contributions to Mineralogy and Petrology*. 2016. Vol. 171. Iss. 10. N 85. DOI: 10.1007/s00410-016-1298-9

34. Pribavkin S.V. Amphibole and biotite of melanocratic rocks from the Ural granitic massifs: composition, relationship, petrogenetic consequences. *Lithosphere* (*Russia*). 2019. Vol. 19. N 6, p. 902-918 (in Russian). DOI: 10.24930/1681-9004-2019-19-6-902-918

35. Ariskin A.A., Barmina G.S., Frenkel M.Y. Simulation of tholeiitic magma crystallization at low pressure with fixed oxygen fugacity. *Geochemistry International*. 1986. Vol. 24. N 5, p. 92-100 (in Russian).

36. Ariskin A.A., Barmina G.S. Modelling of phase equilibria in crystallization of basaltic magmas. Moscow: Nauka, 2000, p. 363 (in Russian).

37. Frenkel M.Ya., Yaroshevskii A.A., Ariskin A.A. et al. Dynamics of in-chamber differentiation of basic magmas. Moscow: Nauka, 1988, p. 216 (in Russian).

38. Nathan H.D., Vankirk C.K. A model of magmatic crystallization. *Journal of Petrology*. 1978. Vol. 19. Iss. 1, p. 66-94. DOI: 10.1093/petrology/19.1.66

39. Puchkov V.N. Geology of the Urals and Ural region (topical issues of stratigraphy, tectonics, geodynamics, and metallogeny). Ufa: DizainPoligrafServis, 2010, p. 280 (in Russian).

***Authors*: Sergey G. Kovalev,** *Doctor of Geological and Mineralogical Sciences, Director, kovalev@ufaras.ru, https://orcid.org/0000-0001-6753-7484* (*Institute of Geology, Ufa Scientific Centre RAS, Ufa, Russia*), **Sergey S. Kovalev,** *Researcher, https://orcid.org/ 0000-0003-1780-6580* (*Institute of Geology, Ufa Scientific Centre RAS, Ufa, Russia*).

The authors declare no conflict of interests.